Biochimica et Biophysica Acta 1864 (2016) 511–522

Contents lists available at ScienceDirect

Biochimica et Biophysica Acta

journal homepage: www.elsevier.com/locate/bbapap

Biochemical, biophysical, and functional properties of ICA512/IA-2 RESP18 homology domain

Laura Sosa [a,b,c,1], Juha M. Torkko [d,e,f,1], María E. Primo [a,b,c], Ramiro E. Llovera [g], Pamela L. Toledo [g,h], Antonella S. Rios [h], F. Luis Gonzalez Flecha [i], Aldana Trabucchi [a,b,c], Silvina N. Valdez [a,b,c], Edgardo Poskus [a,b,c], Michele Solimena [d,e,f], Mario R. Ermácora [g,h,*]

[a] Instituto de Estudios de la Inmunidad Humoral Prof. Ricardo A. Margni (IDEHU), Universidad de Buenos Aires—CONICET, Argentina
[b] Cátedra de Inmunología de la Facultad de Farmacia y Bioquímica, IDEHU, Argentina
[c] División Endocrinología del Hospital de Clínicas José de San Martín, Universidad de Buenos Aires—CONICET, Argentina
[d] Paul Langerhans Institute Dresden, Uniklinikum "Carl Gustav Carus", TU Dresden, Germany
[e] German Center for Diabetes Research (DZD e.V.), Neuherberg, Germany
[f] Max Planck Institute of Molecular Cell Biology and Genetics, Dresden, Germany
[g] Instituto Multidisciplinario de Biología Celular, CONICET, Argentina
[h] Departamento de Ciencia y Tecnología, Universidad Nacional de Quilmes, Argentina
[i] Instituto de Química y Fisicoquímica Biológicas, Facultad de Farmacia y Bioquímica, Universidad de Buenos Aires—CONICET, Junín 956, 1113, Buenos Aires, Argentina

ARTICLE INFO

Article history:
Received 7 September 2015
Received in revised form 4 January 2016
Accepted 29 January 2016
Available online 1 February 2016

Keywords:
ICA512
IA-2
RESP18
Diabetes
Insulin
Protein tyrosine phosphatase

ABSTRACT

Background: ICA512 (or IA-2/PTPRN) is a transmembrane protein-tyrosine phosphatase located in secretory granules of neuroendocrine cells. Previous studies implied its involvement in generation, cargo storage, traffic, exocytosis and recycling of insulin secretory granules, as well as in β-cell proliferation. While several ICA512 domains have been characterized, the function and structure of a large portion of its N-terminal extracellular (or lumenal) region are unknown. Here, we report a biophysical, biochemical, and functional characterization of ICA512–RESP18HD, a domain comprising residues 35 to 131 and homologous to regulated endocrine-specific protein 18 (RESP18).
Methods: Pure recombinant ICA512–RESP18HD was characterized by CD and fluorescence. Its binding to insulin and proinsulin was characterized by ELISA, surface plasmon resonance, and fluorescence anisotropy. Thiol reactivity was measured kinetically. Targeting of ΔRESP18HD ICA512–GFP to the membrane of insulinoma cells was monitored by immunofluorescence.
Results: ICA512–RESP18HD possesses a strong tendency to aggregate and polymerize via intermolecular disulfide formation, particularly at pH > 4.5. Its cysteine residues are highly susceptible to oxidation forming an intramolecular disulfide between cysteine 53 and 62 and intermolecular disulfides via cysteine 40 and cysteine 47. The regulated sorting of ICA512 to secretory granules in INS-1 cells was impaired by deletion of RESP18HD. ICA512–RESP18HD binds with high-affinity to insulin and proinsulin.
Conclusions: RESP18HD is required for efficient sorting of ICA512 to secretory granules.
General significance: RESP18HD is a key determinant for ICA512 granule targeting.

1. Introduction

Receptor-type protein tyrosine phosphatases (RPTPs) constitute a large family of transmembrane proteins involved in signaling pathways [1,2]. There are eight subtypes of RPTP. Members of the R8 subtype, ICA512 (also known as IA-2, PTP35, or PTPRN) and phogrin (also known as IA-2β, IAR, ICAAR, or PTPRN2) have a large ectodomain followed by a single transmembrane segment and a single, catalytically-impaired, protein tyrosine phosphatase (PTP) domain (Fig. 1) [3,4].

ICA512 and phogrin are mainly expressed in neuropeptidergic neurons and peptide-secreting endocrine cells, including insulin-producing pancreatic β-cells. There, they are localized in secretory granules (SGs)

Abbreviations: ICA512, islet cell autoantigen 512; IA-2, insulinoma-associated tyrosine phosphatase 2; RPTP, receptor protein tyrosine phosphatase; RESP18, regulated endocrine-specific protein 18; RESP18HD, regulated endocrine-specific protein 18 homology domain;; GFP, green fluorescent protein; SG, secretory granule; ER, endoplasmic reticulum; ANS, 8-anilino-1-naphthalenesulfonic acid; DTT, dithiothreitol; TNB, 5′-thio-2-nitrobenzoic acid; TMB, 3,3′,5,5′-tetramethylbenzidine; TP, 4-thio pyridine; DTDP, 4,4′-dithiodipyridine; RSTP, thiopyridine mixed disulfide; SPR, surface plasmon resonance.

* Corresponding author at: Departamento de Ciencia y Tecnología, Universidad Nacional de Quilmes, Roque Sáenz Peña 325, 1876 Bernal, Buenos Aires, Argentina.
E-mail address: ermacora@unq.edu.ar (M.R. Ermácora).
[1] These authors contributed equally to this work.

http://dx.doi.org/10.1016/j.bbapap.2016.01.013
1570-9639/

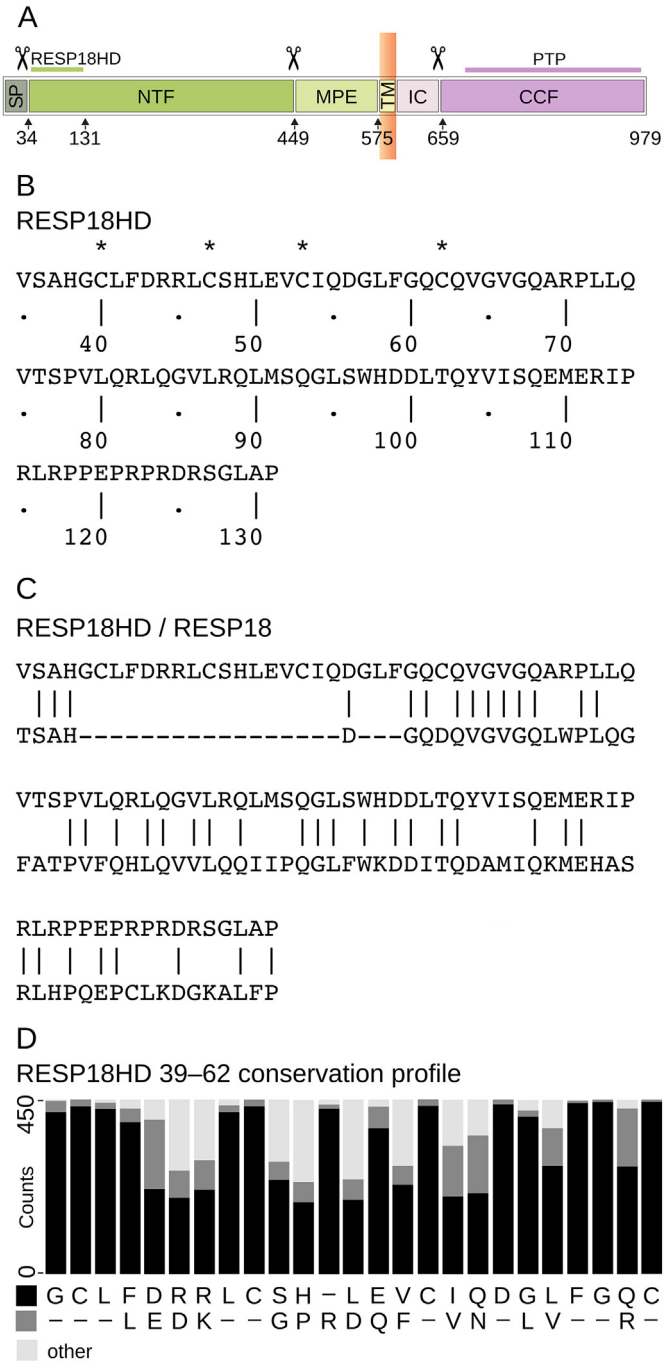

Fig. 1. ICA512 domains and topogenesis. (A) The extracellular segment of ICA512–RESP18HD comprises residues 1–575 and includes a signal peptide (*SP*), the N-terminal fragment (*NTF*), and the Membrane Proximal Ectodomain (*MPE*). The transmembrane domain (*TM*) comprises residues 576–600. The intracellular region, residues 601–979, is made of the juxtamembrane intracellular domain (*IC*) and the Cytoplasmic Cleaved Fragment (*CCF*). Most of CCF corresponds to the pseudo-phosphatase (catalytically inactive) domain (*PTP*), from which the entire protein is named. Scissors mark well-characterized processing sites that produce the mature protein, ICA512–TMF (residues 449–979, corresponding to MPE–TM–IC), which is transiently inserted into the plasma membrane upon exocytosis. (B) The sequence of ICA512–RESP18HD (residues 35–131). Asterisks indicate the four cysteine residues (C40, C47, C53, C62) in this segment. (C) Alignment of ICA512–RESP18HD (top) and human RESP18 (28) (bottom). The two proteins share 53% residue identity in the aligned region. (D) Conservation analysis of the cysteine-rich region of ICA512–RESP18HD. A BLAST search of non-redundant protein data banks using the human sequence 39–62 allowed the identification of 450 homologous. Positive results corresponded to all kind of animals ranging from insects to mammals. The retrieved sequences were aligned and the residue conservation is shown as a bar chart. Cysteine substitution was not observed, and the few instances of cysteine deletion corresponded to isoforms of the receptor in which most of the cysteine-rich region is deleted.

[5,6] and involved in the formation, cargo storage, traffic, exocytosis and recycling of insulin SGs, as well as in β-cell proliferation [4,7–12]. Also, they are prominent type 1 diabetes autoantigens, and autoantibodies elicited by them are widely-used highly-predictive biomarkers for early detection of the disease in relatives and other individuals under genetic risk [5,13,14]. In mice, gene deletion of ICA512, phogrin, or both causes glucose intolerance, decreased glucose-stimulated insulin secretion, abnormal secretion of pituitary hormones, and female infertility [15–17]. Importantly, the insulin granule content of β-cells in ICA512$^{-/-}$ and ICA512$^{-/-}$/phogrin$^{-/-}$ mice is reduced by half [18].

Despite being closely related, phogrin and ICA512 have different expression profiles. ICA512 expression increases during development and is influenced by glucose, insulin, cAMP and cytokines [19–22]. In contrast, phogrin expression is influenced neither by development nor by agents that stimulate insulin secretion [23].

It is believed that ICA512 and phogrin participate in many aspects of the insulin secretory pathway [12], some of which were characterized in detail. Upon removal of its signal peptide, N-glycosylation in the ER, and then O-glycosylation in the Golgi complex, proICA512 [24] is targeted to SGs, where its processing by prohormone convertases generates a 65-kDa transmembrane fragment (ICA512–TMF) and a lumenal N-terminal fragment (ICA512–NTF) (Fig. 1) [5]. Binding of ICA512–TMF to the PDZ domain of β2-syntrophin tethers insulin SGs to actin filaments. The interaction is mediated by utrophin and regulated by phosphorylation/dephosphorylation of β2-syntrophin [11]. During insulin exocytosis, ICA512–TMF is transiently inserted into the plasma membrane, where its cytoplasmic tail is cleaved by the Ca^{2+}-activated protease calpain-1 [7]. The resulting cleaved cytoplasmic fragment (ICA512–CCF) is directed in part to the nucleus, where it binds to the tyrosine phosphorylated signal transducer and activator of transcription STAT5, thereby increasing transcription of insulin and other granule-related genes [25], as well as β-cell proliferation [9]. In the cytosol, on the other hand, the fragment may displace the actin linker β2-syntrophin from its full-length counterpart on the granule, thereby increasing granule mobility and exocytosis [8].

The first 100 residues of ICA512–NTF are homologous to glucocorticoid-responsive protein regulated endocrine-specific protein 18 (RESP18) [26–28], which is expressed in SGs of α, β and δ cells of pancreatic islets [28]. Interestingly, the ICA512 segment homologous to RESP18 (ICA512–RESP18HD) exhibits a conserved cysteine-rich region (residues 39–62), which is absent in RESP18 (Fig. 1). It was demonstrated in our previous work [24] that ICA512–RESP18HD suffices to direct green fluorescent protein (GFP) to insulin SGs, whereas deletion of the entire ICA512–NTF, which includes ICA512–RESP18HD, causes the constitutive delivery of ICA512 to the cell membrane, hence abolishing SG targeting. Moreover, expression of ICA512–NTF tagged with GFP results in ER retention of the fusion protein.

As ICA512–NTF contains a variety of determinants affecting the fate of ICA512, including ER retention and sorting to SGs for regulated exocytosis, insights into its biophysical and structural properties were needed to clarify its function. In this study, therefore, we report the preparation of recombinant ICA512–RESP18HD and its biophysical and biochemical characterization. Availability of purified ICA512–RESP18HD allowed the identification and analysis of its interaction with proinsulin and insulin, which are also reported here. Moreover, we show that deletion of ICA512–RESP18HD alone alters the trafficking of the receptor in insulinoma cells.

2. Materials and methods

2.1. Miscellanea

Dithiothreitol (DTT), diethylene triamine pentaacetic acid (DTPA), lysozyme, and cysteine hydrochloride were purchased from Sigma-Aldrich (San Luis, MO, USA). All other chemicals were of the purest analytical grade available. Human insulin was provided by Laboratorios

Beta S.A. (Buenos Aires, Argentina). Proinsulin was a gift from Eli Lilly (Indianapolis, IN). Thioredoxin was a gift from Dr. Javier Santos (IQUIFIB, UBA–CONICET, Buenos Aires, Argentina). Sodium dodecyl sulfate polyacrylamide gel electrophoresis (SDS-PAGE) was performed as described [29]. A molar absorption coefficient of 7450 M^{-1} cm^{-1} for ICA512–RESP18HD at 280 nm was calculated from the amino acid composition [30]. Electrospray mass analysis was performed on a VG Biotech/Fisons (Altrincham, UK) triple quadrupole spectrometer at the LANAIS–Pro facility, UBA–CONICET, Buenos Aires. Laser desorption mass analysis was performed on a 4800 MALDI TOF/TOF Analyzer from Applied Biosystems, at the Unidad de Bioquímica y Proteómica Analíticas, Pasteur Institut, Montevideo, Uruguay. Dynamic light scattering (DLS) measurements were made on a Zetasizer Nano S DLS device from Malvern Instruments (Worcestershire, UK). 100 μM ICA512–RESP18HD in 6 M urea was diluted to 2 μM ICA512–RESP18HD in 25 mM sodium acetate, pH 4.5, or 25 mM HEPES, pH 7.0. Samples were incubated at 20 °C for 1 h and filtered with Ultrafree-MC microcentrifuge filters (0.22 μm; Millipore) before measurement. Time-course aggregation experiments followed by light scattering and as a function of pH were performed similarly to the above DLS experiments, except that the final pH of the solution was 4–7.0, as required, and the filtration step was omitted before UV scatter measurement at 400 nm. Isothermal microcalorimetry was carried out with a MicroCal VP–ITC calorimeter (Malvern Instruments, Worcestershire, UK). Least squares fitting and simulations were carried out with *R* [31].

2.2. Molecular biology

The cDNA encoding ICA512–RESP18HD was prepared using primers forward 5′-CATATGGTTAGTGCACACGGCTGTCTATTTG-3′ and reverse 5′-GGATCCTCAGGGTGCCAAGCCAGAC-3′. The properly flanked cDNA for ICA512–RESP18HD was cloned into pGEM–T Easy vector (Promega, Madison, USA). Subsequently, a fragment was excised with NdeI and BamHI and subcloned into pET-9b (Novagen, Madison, USA) to yield pET-9 ICA512–RESP18HD (amino acid residues 35–131).

The pEGFP-N1 construct for expression in rat insulinoma (INS-1) cells of full length ICA512 (amino acid residues 1–979, Uniprot entry: PTPRN_HUMAN) fused at its C terminus to GFP was described previously [24]. The pEGFP-N1 expression construct for ΔRESP18HD ICA512–GFP (amino acid residues 134–979) was fused at its N- and C-termini to the CD33 signal peptide sequence and to GFP, respectively. Site-directed mutagenesis was performed with a QuikChange kit (Stratagene). All construct sequences were confirmed by DNA sequencing.

2.3. Protein expression and purification

Escherichia coli BL21 (DE3) pLysS cells transformed with pET-9 ICA512–RESP18HD were cultured at 37 °C in 250 ml Luria–Bertani medium supplemented with 50 μg/ml kanamycin and 34 μg/ml chloramphenicol to $A = 1.0$ at 600 nm. Protein expression was induced with 1 mM isopropyl β-D-1-thiogalactopyranoside (Fluka, Buchs, Switzerland). After a 4-h induction, bacteria were harvested by centrifugation, resuspended in 10 ml of lysis buffer (100 mM NaCl, 5 mM EDTA, 1 mM DTPA, 5 mM DTT, 5 mM β-mercaptoethanol, 50 mM Tris–HCl, pH 7.8), and broken by high pressure (3000 psi) with a French Press (Spectronics Instruments, Rochester, NY, USA) or by sonication using a tip sonicator (6 pulses, 200 joules, 5 watts, on a ice bath). As ICA512–RESP18HD expression resulted mostly in the generation of inclusion bodies, the insoluble fraction was collected by centrifugation (12,000 × *g*, 15 min, 4 °C). To purify the inclusion bodies from associated impurities, the insoluble fraction was resuspended by sonication in lysis buffer containing 0.2% deoxycholic acid and recovered by centrifugation as above three times. Then, lysis buffer was removed by washing once with water.

The isolated inclusion bodies were solubilized by incubation (1 h, 37 °C) with 6 M urea, 25 mM sodium acetate, 10 mM glycine, 5 mM tris(2-carboxyethyl)phosphine, pH 4.5, and subjected to ion-exchange chromatography on a Hiprep SP (GE Healthcare) column equilibrated at 20 °C with 6 M urea, 25 mM sodium acetate, 10 mM glycine, pH 4.5. Pure ICA512–RESP18HD was obtained by elution with a salt gradient (0–1.0 M NaCl in equilibration buffer).

Oxidative refolding of ICA512–RESP18HD was carried out by dialysis, with a redox buffer system containing 20 mM Tris–acetic acid pH 4.5, 10 mM β-mercaptoethanol, 3,3′-dithiodipropionic acid, 0.5 mM cystamine, and 0.5 mM cystine. Non-oxidative refolding was performed by size-exclusion chromatography on a HiTrap desalting column (GE Healthcare) equilibrated in 20 mM Tris–acetic acid pH 4.5. Identity and integrity of purified ICA512–RESP18HD were confirmed by electrospray mass analysis.

2.4. Circular dichroism

CD spectra were collected at 20 °C on a Jasco 810 spectropolarimeter (Jasco Corporation, Tokyo, Japan). Far-UV CD spectra were scanned from 185 to 340 nm with a 0.1-cm cell and 10-μM protein concentration. For near-UV CD spectra, wavelength range, protein concentration and path length were 240–340 nm, 50 μM, and 1.0 cm, respectively. Scan speed was set to 20 and 50 nm/min (near-UV and far-UV, respectively) with 1-s response time, 0.2-nm data pitch and 1-nm bandwidth. Eight to ten scans were averaged for each sample, blank subtracted, and smoothed using a fourth-degree Savitzky–Golay polynomial filter with a 10-point sliding window.

2.5. Fluorescence measurements

Steady-state fluorescence measurements were performed on an ISS K2 multifrequency phase fluorometer (ISS, Champaign, Illinois, USA) equipped with a cell holder connected to a circulating water bath at 20 °C and 1.0-cm cells. The excitation wavelength was 295 nm, and the spectral slit width was 3 nm.

For binding experiments, 2 μM ICA512–RESP18HD in 25 mM sodium acetate, pH 4.5 was incubated 5 min at room temperature with 50 μM 8-anilino-1-naphthalenesulfonic acid (ANS). As a control, 50 μM ANS in the same buffer was measured. The excitation wavelength was at 350 nm and the emission was measured between 400 and 600 nm.

Anisotropy measurements of the interaction of insulin and ICA512–RESP18HD were carried out with a SLM–Aminco Bowman Series 2 spectrofluorometer (SLM, Urbana, IL, USA). Polarized excitation and emission were 297 and 340 nm, respectively. The bandwidth was 4 and 8 nm for excitation and emission, respectively. ICA512–RESP18HD was 47 μM in the presence of 0–250 μM insulin. Fluorescence anisotropy was calculated as $r = (I_{||} - I_{\perp}) / (I_{||} + 2I_{\perp})$, where the subscripts indicate vertically (||) and horizontally ($\perp$) polarized emission.

2.6. Immunochemical procedures

A polyclonal antibody to ICA512–RESP18HD was obtained by immunizing New Zealand White rabbits with 0.1 mg of antigen emulsified in complete Freund's adjuvant. The initial injection was followed by booster injections with 0.1 mg of antigen in incomplete Freund's adjuvant at 3-week intervals. Blood collection was carried out 15 days after the booster injection. The immunoreactivity of the obtained antibodies was tested by ELISA, using ICA512–RESP18HD coated polystyrene plates.

The interaction between ICA512–RESP18HD and insulin or proinsulin was measured by ELISA at room temperature, in 50 mM sodium acetate, pH 4.5. Dilutions of 2 μg/ml ICA512–RESP18HD were incubated 1.5 h on polystyrene wells previously coated with 50 ng of insulin or proinsulin. After washing with incubation buffer, the formation of the complexes was revealed by incubation with the rabbit polyclonal antibody in 137 mM NaCl, 2.7 mM KCl, 10 mM Na2HPO4, 1.8 mM KH2PO4, pH 7.4 (PBS), followed by a 1.5-h incubation with a secondary anti-rabbit IgG–peroxidase conjugate (Jackson ImmunoResearch

Laboratories, West Grove, PA, USA), and standard color development procedures with the chromogenic substrate 3,3′ 5,5′-tetramethylbenzidine. The extent of the interaction was measured by UV absorption at 450 nm. Two control assays were performed: (i) ICA512–RESP18HD dilution was replaced by incubation buffer, and (ii) the rabbit polyclonal serum was replaced by rabbit pre immunization serum.

2.7. Cell culture, expression and immunostaining in INS-1 cells

Insulinoma INS-1 cells were transfected with the pEGFP-N1, ICA512–GFP or ΔRESP18HD ICA512–GFP constructs, plated onto coverslips on 35-mm culture dishes, and grown for 4 days in standard RPMI 1640 medium. Then, for the fusion proteins expression, the culture medium was replaced by resting buffer (2.8 mM glucose, 5 mM KCl, 120 mM NaCl, 24 mM NaHCO3, 1 mM MgCl2, 2 mM CaCl2, 1 mg/ml ovalbumin, 5 mM HEPES, pH 7.5) for 1-h pre incubation. Next, cells were incubated for 2 h in resting or stimulation buffer (25 mM glucose, 55 mM KCl in 70 mM NaCl, 24 mM NaHCO3, 1 mM MgCl2, 2 mM CaCl2, 1 mg/ml ovalbumin, 5 mM HEPES pH 7.5), and rinsed three times in PBS. Cells were washed twice in ice-cold PBS and harvested in ice-cold lysis buffer, with 20 mM Tris–HCl, pH 8.0, 140 mM NaCl, 1 mM EDTA, 1 mM Triton X–100, 1% protease inhibitor cocktail (Sigma). Cell lysates were centrifuged for 15 min, 12,000 rpm at 4 °C, and the precleared soluble protein fractions was prepared in SDS-PAGE sample buffer, heated to 95 °C for 5 min and subjected to SDS-PAGE and Western blotting analysis with a mouse GFP antibody (Clontech, cat. #632381). A gamma tubulin antibody (Sigma, cat. #T6557) was additionally employed for a sample loading control.

For insulin antibody immunostaining, cells (at rest or stimulated) were fixed with 4% paraformaldehyde. Aldehyde quenching/permeabilization was performed with 200 mM glycine, 0.1% Triton X–100 in PBS for 20 min, after which cells were incubated in blocking buffer 0.2% gelatin, 0.5% albumin in PBS for 1 h. The cells were then incubated in blocking buffer with a guinea pig anti-insulin antibody (Abcam, cat. #ab7842) at 4 °C overnight, rinsed five times with PBS, and incubated in blocking buffer with goat anti-guinea pig Alexa Fluor 568-conjugated antibodies for 2 h at room temperature. For live cell staining, the cell culture dishes after the 1 h preincubation were cooled on ice, and the cells were incubated with resting or stimulation buffer, supplemented with mouse ICA512 ectodomain ME ICA512 antibody (directed against an epitope within amino acid residues 449–575) [24]. To prevent the antibody internalization, the cells were incubated for 20 min at 4 °C, rinsed three times in PBS and fixed with 4% paraformaldehyde. Omitting the permeabilization step, the cells were then incubated for 1 h in blocking buffer (0.2% gelatin, 0.5% albumin in PBS) and then for 2 h in blocking buffer with goat anti-mouse, Alexa Fluor 568 conjugated antibodies at room temperature. Finally, cells were rinsed five times in PBS and the coverslips were mounted onto slides with Mowiol®. Images were acquired with an Olympus FluoView–1000 laser scanning confocal microscope equipped with a 60× PlanoApo OLSM lens (NA = 1.10).

2.8. Thiol reactivity analysis

The kinetics of the reaction at pH 4.5 between thiol groups and 5,5′-dithiobis-(2-nitrobenzoic acid (DTNB) or 4,4′-dithiodipyridine (DTDP) was monitored measuring changes in UV absorption due to the variation in the concentration of 5′-thio-2-nitro-benzoic acid (TNB), 4-thio pyridine (TP), DTDP, and thiopyridine mixed disulfide (RSTP). The molar extinction coefficient of TNB at pH 4.5 was $\varepsilon_{412\ nm} = 6{,}980\ M^{-1}\ cm^{-1}$ (our own determination, not shown). The molar extinction coefficient at pH 4.5 of TP, DTDP, and RSTP were 21,400, 1000, and 500 $M^{-1}\ cm^{-1}$, respectively [32].

Besides ICA512–RESP18HD, the reaction was carried out with cysteine, thioredoxin, and lysozyme. Previously, the proteins were fully reduced with DTT and rendered free of the reducing agent by size exclusion chromatography.

The reaction with DTNB at pH 4.5 was sufficiently slow as to permit manual mixing and pseudo-first-order conditions (large excess of DTNB), and therefore standard integrated kinetic equations and least squares fitting were used to estimate rate constants. Moreover, the reaction of an excess of DTNB with free thiol groups was assumed to be limited to

$$RS^- + DTNB \rightarrow RSSNB + TNB,$$

and second-order constants were calculated as $k = k_{obs} / [DTNB]$, where k_{obs} represents the apparent pseudo-first-order constant of the kinetic reaction.

In the case of DTDP, the reaction was much faster and the reagent concentration had to be kept low. Moreover, a two-step reaction mechanism needed to be considered:

$$RS^- + DTDP \rightarrow RSTP + TP,$$

$$RS^- + RSSP \rightarrow RSSR + TP.$$

This forced us to use the kinetic equations for second-order reactions in their differential forms. The rate constants were estimated by two procedures: (*i*) an *R* script was written to simulate the reaction, and, starting from initial guesses, the rate constants were changed by trial-and-error until a good fit of the simulated curve to the experimental data was achieved; (*ii*) using the method of Runge Kutta implemented in *R*. The two approaches led to concordant estimates.

2.9. Surface plasmon resonance (SPR)

Real-time insulin binding experiments were carried out with a SPR BIAcore T100 biosensor (BIAcore, GE Healthcare, Uppsala, Sweden) on a carboxymethylated-dextran CM5 sensor chip surface (GE Healthcare, Uppsala, Sweden) with immobilized insulin or proinsulin. Covalent attachment to the chip surface was achieved by activating its carboxyl groups with 1-ethyl-3-(3-dimethylaminopropyl) carbodiimide and N-hydroxysuccinimide. The extent of the immobilization resulted in cell signals of approximately 800 resonance units. Assays were run at 20 °C whit a flow rate of 10 μl/min. Binding rates were measured after injecting for 120 s different ICA512–RESP18HD dilutions in 20 mM sodium acetate, pH 4.5. Desorption rates were measured passing over injection buffer. After each sample application, a regeneration step was carried out passing over 10 mM glycine-HCl, pH 1.5. All sensorgrams were corrected by subtracting the signal from the reference flow cell. To measure the affinity of specific binding between ICA512–RESP18HD and insulin or proinsulin, a 1:1 binding model ($A + B \rightleftarrows AB$) was used. The association rate constant (k_a), the dissociation rate constant (k_d), and the equilibrium constant (K_D), were calculated by nonlinear least-squares fitting of the model to the data from the sensorgrams using the built-in equations of BIA-evaluation software applicable to the binding model.

3. Results

3.1. Preparation of ICA512–RESP18HD

Several attempts to express the entire ICA512–NTF sequence (Fig. 1) as a recombinant protein in *E. coli* were unsuccessful (not shown) because the yield was very low and the purification unsatisfactory. After testing different constructs, it was found that the N-terminal region of ICA512–NTF, comprising residues 35 to 131 (ICA512–RESP18HD; Fig. 1), could be expressed with good yield and was more tractable, and therefore this study focused on it.

ICA512–RESP18HD expressed in *E. coli* appeared predominantly in inclusion bodies. Insoluble ICA512–RESP18HD contained moderate

amounts of disulfide-linked chains (Fig. 2, Panel C, lanes 4 and 5). Urea-solubilization, purification under denaturing conditions, and refolding at pH 4.5 allowed the recovery of large amounts of pure and soluble ICA512–RESP18HD.

The acidic condition was essential for purification since the protein rapidly aggregated and precipitated at neutral pH. This behavior reflects the charge vs. pH profile of the protein: at pH 4.5 the net charge calculated from the sequence is +7.5, whereas at pH 7.5 the value drops to +0.6. Besides, when ICA512–RESP18HD was purified in the absence of strong reducing agents, or when the refolding of the urea-denatured purified protein was carried out under conditions that promote oxidation, a larger proportion formed disulfide-linked oligomers (Fig. 2, Panel B, lane 2).

Mass analysis of the purified protein was in agreement with the expected sequence within experimental error (Fig. 1). However, it also showed that a significant fraction of the protein retained the N-terminal translation-initiator methionine residue.

The aggregation behavior of purified ICA512–RESP18HD was further investigated by DLS (Fig. 3, Panel A). At pH 4.5, fully reduced ICA512–RESP18HD self associated. The most prominent aggregation states at this pH were those with 2–16 associated monomers. At pH 7.0, the population of associated molecules shifted to very large aggregates ($n > 500$). The oxidatively refolded protein at acidic pH populated intermediate high-order aggregates ($n = 16$–256). Thus, although oxidation promoted further aggregation the tendency to associate was independent of it.

The time course and pH dependence of ICA512–RESP18HD aggregation was easily monitored by UV light scattering at 400 nm (Fig. 3, Panel B). It was found that aggregation is not significant at pH < 5.5 and that aggregation rates increase as a function of pH in the 6–7.0 range. Non-reducing SDS-PAGE analysis of samples precipitated by TCA at the end of the kinetic measurements indicated that at pH 7.0 high-order disulfide-linked aggregates were only slightly increased (not shown).

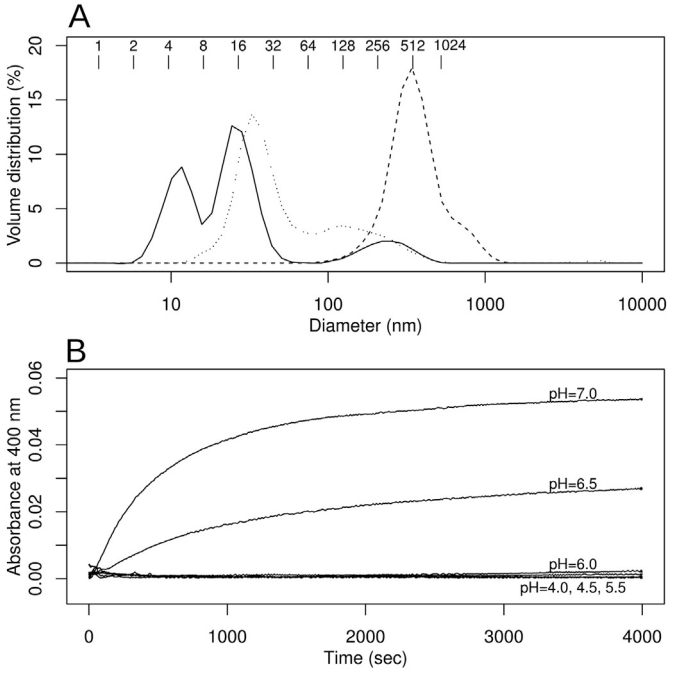

Fig. 3. Aggregation state of ICA512–RESP18HD. (A) The distribution of particle size, assuming spherical shape and weighted by volume, was measured by DLS. The number of associated chains in the multimers (inset ruler) was estimated using the relationship between Stokes radius and molecular weight for native proteins reported in Ref. [49]. Unfolded and fully reduced ICA512–RESP18HD in 6 M urea was refolded by dilution at pH 4.5 or pH 7.0 (see Materials and methods) before measurement. Most of the aggregates populated at acidic pH (solid line) correspond to n-mers with $n = 2$–16. At neutral pH (dashed line), very large aggregates were formed. Oxidatively refolded protein at pH 4.5 showed an intermediate behavior (dotted line). (B) The time curse of the pH-induced aggregation of ICA512–RESP18HD was monitored by light-scattering at 400 nm. At time zero, urea-denatured samples in buffer 25 mM sodium acetate, pH 4.5 were diluted to 2 μM protein in acetic acid–HEPES buffer adjusted to the indicated pH.

3.2. Conformational analysis

The degree of structural organization of refolded ICA512–RESP18HD at pH 4.5 was assessed by near- and far-UV CD (Fig. 4). As a control, the spectra of ICA512–RESP18HD populated under highly-acidic unfolding conditions (20 mM HCl) were acquired. In the near-UV, strong negative bands in the aromatic region (260–300 nm) evidenced the presence of significant tertiary structure in refolded ICA512–RESP18HD; a much less pronounced signal was indicative of absence of defined structure in the unfolded control. In the far-UV, the spectrum of unfolded ICA512–RESP18HD displayed the typical features of random coils: a strong minimum at 200–205 nm and a maximum well beyond 190 nm. Contrastingly, refolded ICA512–RESP18HD exhibited minima in the 208–220 nm region and a maximum around 190 nm, consistently with the presence of significant amounts of secondary structure.

The presence of tertiary structure was also suggested by fluorescence experiments. Judging from the maximum of fluorescence emission, the single ICA512–RESP18HD tryptophan residue was in a hydrophobic environment at pH 4.5. Urea-induced unfolding shifted

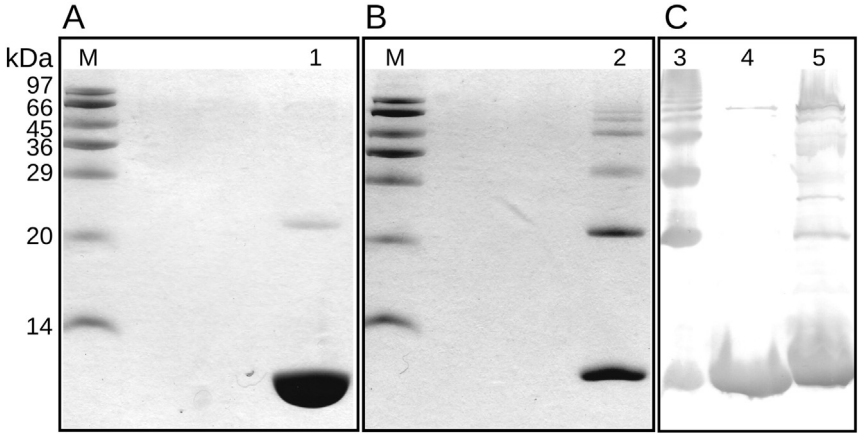

Fig. 2. Oligomerization analysis of ICA512–RESP18HD. (A) SDS-PAGE of pure ICA512–RESP18HD reduced with 2% 2-mercaptoethanol (lane 1) and molecular weight markers (lane *M*). (B) SDS–PAGE of pure ICA512–RESP18HD after oxidative refolding (see Materials and methods) (lane 2) and molecular weight markers (lane *M*). (C) Western blot of pure ICA512–RESP18HD after oxidative refolding (lane 3); pure ICA512–RESP18HD reduced with 2% 2-mercaptoethanol (lane 4); inclusion bodies from *E. coli* expressing ICA512–RESP18HD without reduction (lane 5).

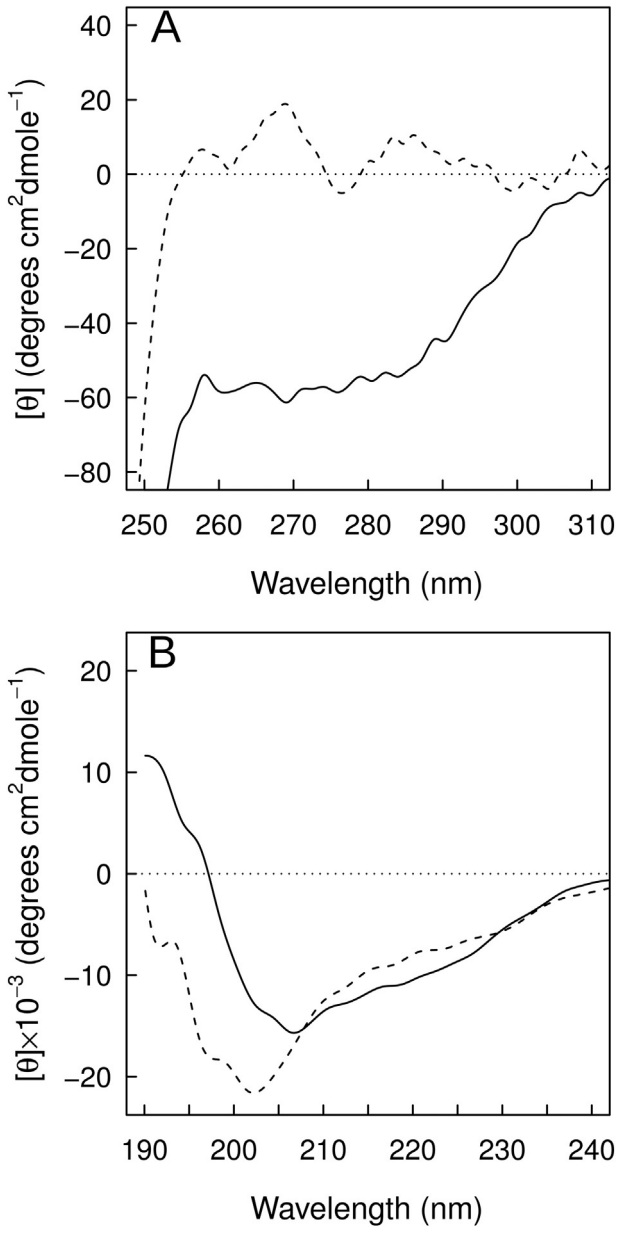

Fig. 4. CD spectra. (A) Near-UV and (B) far-UV CD spectra of ICA512–RESP18HD. Samples were dissolved in 2.5 mM sodium acetate, pH 4.5 (full lines) or in 2.5 mM sodium acetate, 20 mM HCl (dotted lines).

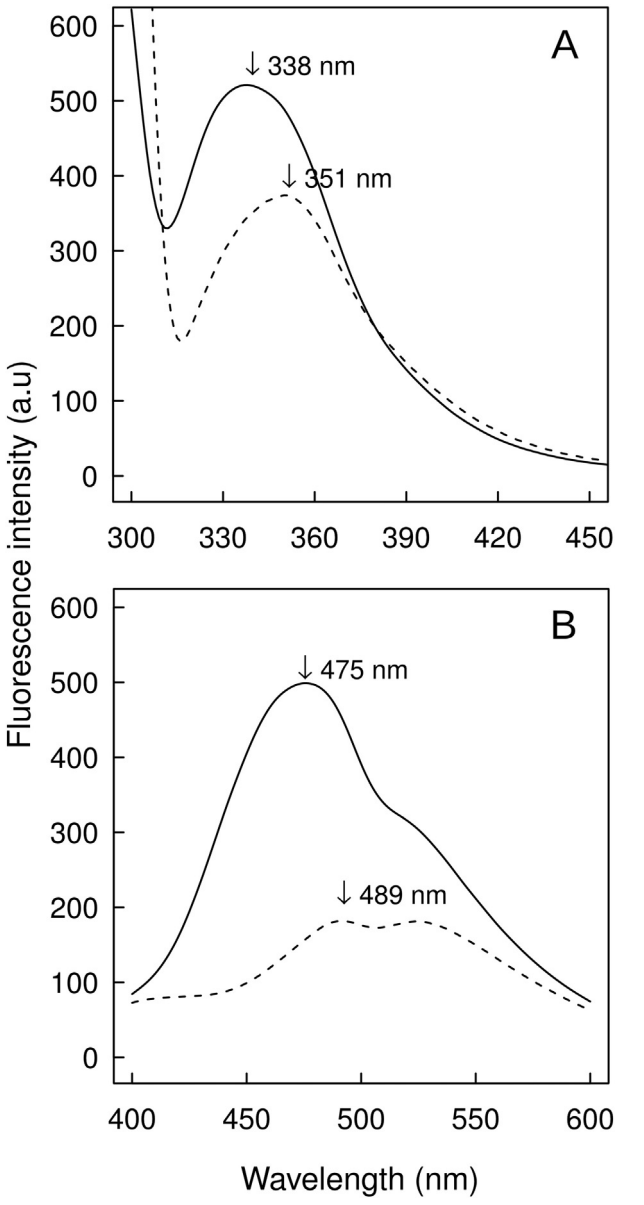

Fig. 5. Fluorescence emission spectra of ICA512–RESP18HD and its ANS complex. (A) 2 μM ICA512–RESP18HD in 25 mM sodium acetate, pH 4.5 (full line) and in the same buffer containing 6 M urea (dashed line). The red shift brought about by unfolding is indicated. (B) 50 μM ANS in 25 mM sodium acetate, pH 4.5 (dashed line) and 50 μM ANS plus 2 μM ICA512–RESP18HD in the same buffer (full line). The large blue shift and increase in quantum yield brought about by the ANS binding to hydrophobic patches in ICA512–RESP18HD is shown.

the emission maximum to the typical emission wavelength of solvated tryptophan residues and decreased the quantum yield, as expected for an unfolding transition (Fig. 5, upper panel).

Although the CD and fluorescence spectra unequivocally showed the presence of tertiary structure, side-chain packing in ICA512–RESP18HD may be less tight than in typical native proteins. ANS binding to ICA512–RESP18HD was clearly revealed by the emission spectra of bound and unbound dye (Fig. 5, lower panel). Binding of ANS is considered diagnostic of partially folded states, or of folded states with extensive packing defects that result in the exposure of hydrophobic patches [33].

3.3. Intrinsic disorder and aggregation propensity

Formation of significant amounts of precipitated material from stock solutions stored frozen or a 4 °C for 1–2 weeks evidenced a conformational instability of ICA512–RESP18HD. SDS-PAGE indicated that the insoluble aggregate contained a large proportion of disulfide-linked, oligomerized material (not shown). The tendency to aggregation and oxidation was observed even in concentrated urea solutions. Taking the above results into account, the experiments were always performed with freshly prepared protein stocks.

The propensity to aggregate exhibited by ICA512–RESP18HD may be due to specific sequence determinants. We analyzed the sequence in search of regions with intrinsic propensity to disorder and found that residues 109–131, i.e. the last 23 residues, scored positive with the predictor implemented in The Database of Protein Disorder (DisProt), a curated database of proteins that lack fixed 3D structure, locally or entirely, in their putative native states [34]. The algorithm also identified intrinsically disordered stretches in cognate regions of phogrin and RESP18.

3.4. Thiol reactivity

Reactivity of ICA512–RESP18HD cysteine residues at pH 4.5 was compared with that of cysteine, a model compound for solvent-exposed protein thiol groups, and with that of fully-reduced thioredoxin and lysozyme, two proteins possessing highly-reactive cysteine residues [35,36]. Thiol reactivity was assessed measuring second order rate constants of the reaction with DTNB and DTDP (Table 1).

DTNB reacted with ICA512–RESP18HD and lysozyme one hundred times faster than with cysteine, and the same reaction with thioredoxin was a thousand times faster. DTDP reacted with thioredoxin, ICA512–RESP18HD, and lysozyme thirteen, ten, and three times faster than with cysteine, respectively. These results unveiled the high reactivity of ICA512–RESP18HD in thiol-disulfide exchange reactions and provided an explanation for its strong tendency to undergo cysteine oxidation, even under acidic conditions that normally would prevent thiol oxidation and formation of disulfides.

3.5. Intra- and intermolecular disulfide bridges

Since native oxidative refolding after purification exacerbated the formation of disulfide-linked oligomers (Fig. 2) and there are four cysteine residues in ICA512–RESP18HD (Fig. 1, Panel D), we undertook the identification of those involved in the formation of disulfide bridges. The aggregation propensity and thiol reactivity of the protein made the analysis quite difficult. However, different aggregation states could be isolated by SDS-PAGE and in-gel digested with trypsin and endoproteinase Glu-C, with and without a pretreatment with DTT, 4-vinylpyridine, and/or iodoacetamide. The resulting peptides were analyzed by mass spectroscopy. A large set of data was collected, and some of the more relevant results are shown in Table 2. Based on the comparison of the results for monomer and oligomers, and for the different treatments, we conclude that ICA512–RESP18HD readily forms an intramolecular disulfide linking Cys 53 and Cys 62. On the other hand, Cys 40 and Cys 47 were found either reduced or forming intermolecular disulfides in the oligomerized states, although a low-yield formation of an intramolecular sulfur–sulfur bond between them could not be ruled out. The analysis also highlighted the extreme susceptibility of ICA512–RESP18HD to oxidative damage, as many different products of reactive-oxygen species attack could be identified (particularly as methionine sulfoxide and sulfone derivatives).

3.6. Interaction of ICA512–RESP18HD with insulin and proinsulin

Since the ICA512 ectodomain in vivo is in the proximity of large amounts of insulin and proinsulin, the possible association between the two proteins through ICA512–RESP18HD was investigated. To that end, a variety of analyses, based on different physicochemical principles, were performed to assess specific binding in vitro.

Fluorescence anisotropy is based on the dependence of polarized fluorescence emission with the apparent hydrodynamic size of bound and unbound ligands. Complexes are larger in size and have smaller rotational diffusion coefficients than free ligands, and thus bound ligands exhibit higher polarized fluorescence emission than free ligands. As shown in Fig. 6, fluorescence measurements of ICA512–RESP18HD at pH 4.5 after excitation of its single tryptophan residue in the presence of insulin in the micromolar range revealed a dose-dependent increase of anisotropy consistent with the formation of a complex and concomitant decrease of the rotational diffusion of ICA512–RESP18HD (human insulin contains no tryptophan residues).

Another general approach for the analysis of protein–protein interactions is isothermal titration calorimetry (ITC). Using a computer-controlled mixing device, extremely sensitive temperature sensors and sophisticated instrumentation, the formation of a complex can be detected and quantified by the heat absorbed or released during the reaction. By this technique, an exothermic reaction between ICA512–RESP18HD and insulin was readily detected; however the heat release was too large and slow to be accounted for by a simple bimolecular association process, and a suitable model could not be found to estimate thermodynamic parameters (not shown).

Since neither the fluorescence anisotropy nor the ITC experiments gave typical saturation curves, the affinity equilibrium constant based on the Law of Mass Action could not be estimated. Therefore, two alternative procedures were used to assess the strength of the interaction: SPR and ELISA. In a typical SPR experiment, one of the ligands is chemically immobilized on a surface while a solution containing the other flows continuously over it. Binding is evidenced by optical effects induced by light stimulation of the metallic support of the binding surface. When the sample solution is replaced by buffer, the response decreases

Table 1
Second-order rate constants for thiol-disulfide exchange reactions[a].

Thiolate	disulfide	k (M^{-1} s^{-1})[b]
ICA512–RESP18HD	DTNB	107 ± 3.5
Thioredoxin	DTNB	907 ± 81
Lysozyme	DTNB	116 ± 12
Cysteine	DTNB	1.64 ± 0.5
ICA512–RESP18HD	DTDP	5000 ± 424
Thioredoxin	DTDP	6900 ± 737
Lysozyme	DTDP	1530 ± 205
Cysteine	DTDP	535 ± 35

[a] At 20 °C in 25 mM sodium acetate, pH 4.5.
[b] Mean ± SD of two or more experiments.

Table 2
Mass analysis of selected ICA512–RESP18HD proteolytic fragments[a].

	Experimental (*m/z*)	Calculated (*m/z*)	Assignment (residues)	Observations
1	2658.16	2658.26	46–70	C47–C53 or C47–C62 or C53–C62
2	2660.19	2660.26	46–70	DTT treatment of (*1*)
3	1235.57	1234.55	34–44	Initial Met not removed, C40SH
4	857.43	857.42	45–51	V8 + trypsin, C47SH
6	1975.97	1975.95	52–70	V8 + trypsin, C53–C62

[a] Only a small subset of representative data are listed. SDS-PAGE bands of monomeric, dimeric and trimeric ICA512–RESP18HD were digested *in gel* with trypsin, V8 protease, or both. In turn, samples were analyzed with and without DTT reduction, and with and without treatment with 4-vinylpyridine or iodoacetamide.

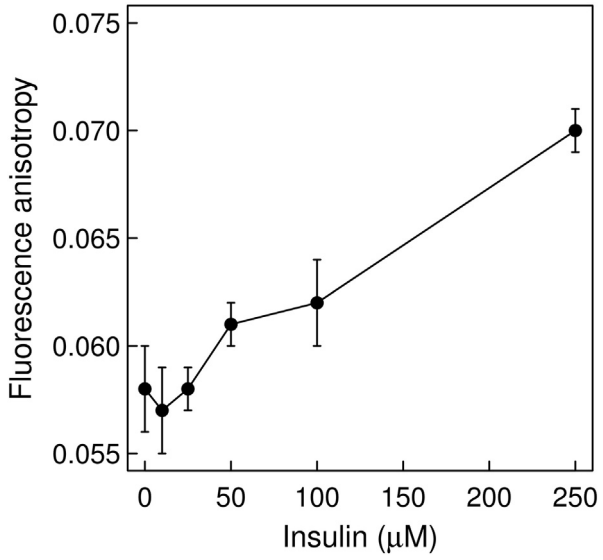

Fig. 6. Fluorescence anisotropy of the interaction between ICA512–RESP18HD and insulin. The vertically and horizontally polarized fluorescence emission from the single tryptophan residue of ICA512–RESP18HD was measured (human insulin contains no tryptophan residues) to calculate anisotropy as described in Materials and methods.

as the interacting partners dissociate. Thus, in this analysis, affinity is not measured at equilibrium, but estimated indirectly from a kinetic measurement. For a simple 1:1 interaction, the equilibrium constant K_D is the ratio of the kinetic rate constants, k_d/k_a. To estimate the affinity of the complex formed by ICA512–RESP18HD and insulin or proinsulin, these ligands were chemically linked to the chip surfaces, and the experiments were conducted at pH 4.5 with ICA512–RESP18HD in its reduced form. The results of the assay are shown in Fig. 7. The SPR apparent K_D for insulin and proinsulin were 104 and 48.1 nM, respectively. In addition, the experiments demonstrated that the interaction is not mediated by the formation of disulfides, since the simple injection of non-reducing buffer induced a significant dissociation of the formed complex.

Finally, to assess binding under non equilibrium conditions, we resorted to ELISA. This method is based on the immobilization of one of the ligands onto a solid surface by irreversible absorption (coating). In a second step the other ligand in solution is incubated with the coated surface, allowing the formation of an irreversible complex. After washing away unbound ligands, the amount of formed complex is quantified with specific antibodies and antibody antibody–enzyme conjugates to amplify a measurable signal from the final multicomponent complex. The experimental variables of an ELISA are optimized until the assay is rendered specific for the complex of interest. Optimization is achieved by lowering the concentrations of ligands and antibodies until only the absorption driven by high-affinity interactions remains. We developed a specific ELISA to assess the interaction between ICA512–RESP18HD and insulin or proinsulin. In this assay insulin or proinsulin absorbed onto polystyrene wells were incubated with high dilutions of ICA512–RESP18HD. The formation of the complex was revealed by successive reactions with a rabbit polyclonal antibody specific for ICA512–RESP18HD, followed by a secondary anti-rabbit IgG–peroxidase conjugate, and an enzyme linked chromogenic assay. The results are shown in Fig. 8. Two controls excluded the possibility of non-specific interactions: (a) reactions in which the specific rabbit polyclonal anti-ICA512–RESP18HD antibody was replaced by pre immunization rabbit serum (inset to Fig. 8, bars labeled *R*); (b) reactions

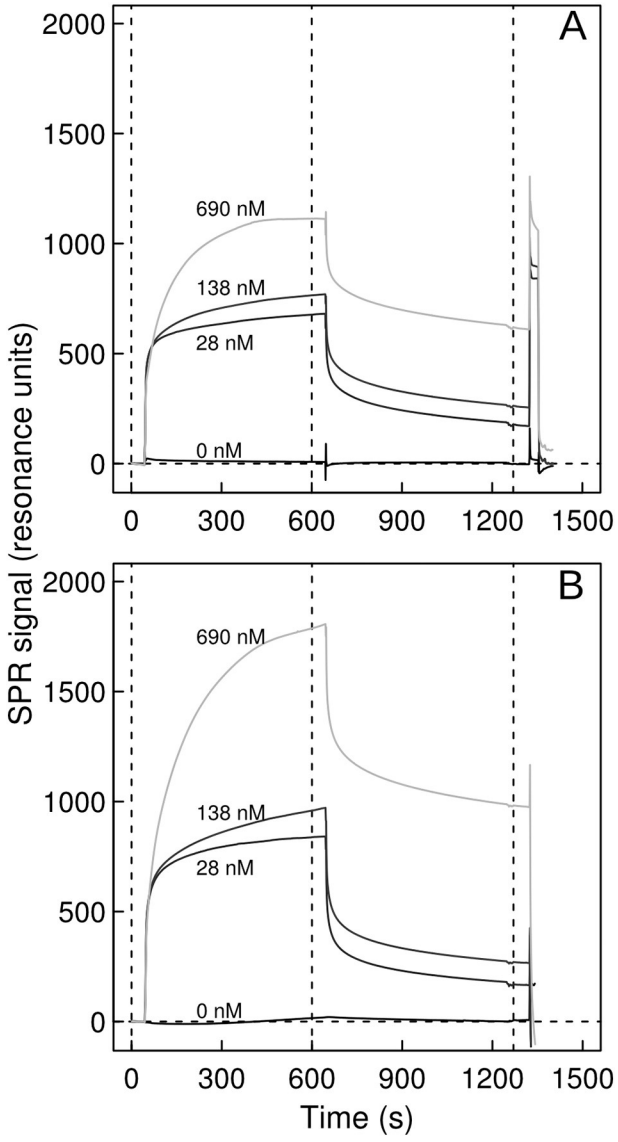

Fig. 7. SPR sensorgrams for ICA512–RESP18HD binding to (A) immobilized proinsulin or (B) insulin. Representative experiments are shown. The indicated concentrations of ICA512–RESP18HD were injected to interact with insulin or proinsulin immobilized on the biosensor chip (see Materials and methods). From left to right, vertical dot lines delimit the injection, desorption, and regeneration times, respectively.

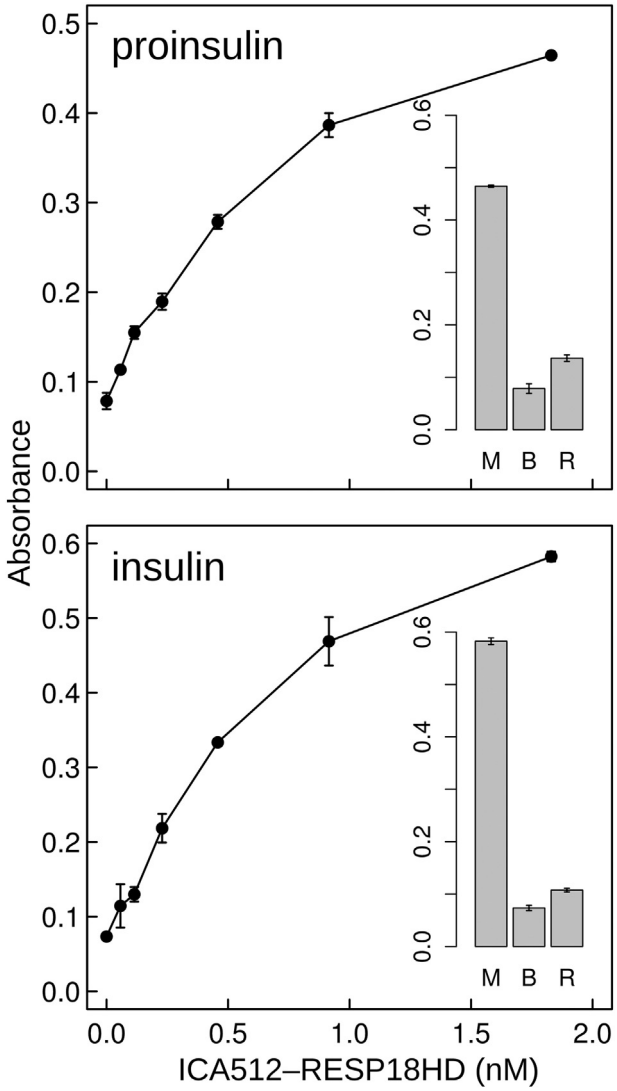

Fig. 8. ELISA of ICA512–RESP18HD interaction with insulin and proinsulin. ICA512–RESP18HD at the indicated concentrations was incubated at pH 4.5 in polystyrene wells coated with 50 ng of insulin or proinsulin. The formed complexes were revealed by successive reactions with a rabbit polyclonal antibody to ICA512–RESP18HD, anti rabbit IgG–peroxidase, and TMB. Absorbance at 450 nm is shown. The bar plots in the insets show the controls performed. Bars labeled *M* correspond to the signal for the highest assayed concentration of ICA512–RESP18HD (1.83 nM). Bars labeled *B* show the signal for reactions with buffer (0 nM ICA512–RESP18HD). Bars labeled *R* represent the signal for the reactions in which rabbit pre-immunization serum replaced the rabbit polyclonal antibody. Error bars indicate the *SD* of duplicates.

with no ICA512–RESP18HD added (inset to Fig. 8, bars labeled *B*). Both controls yielded similarly low signals, much lower than the positive control (inset to Fig. 8, bars labeled *M*). Several nanomolar concentrations of ICA512–RESP18HD were assayed, and typical dose–response curves were obtained for both, insulin and proinsulin. In agreement with the SPR experiment, the range of concentrations at which ICA512–RESP18HD binding was observed is compatible with an interaction of high affinity.

3.7. Expression and cell surface targeting of ΔRESP18HD ICA512–GFP in INS-1 cells

To directly assess the role of ICA512–RESP18HD in the processing and progression of ICA512 in the secretory pathway, we generated a construct, ΔRESP18HD ICA512–GFP, in which the RESP18HD region was eliminated. Full-length ICA512–GFP and ΔRESP18HD ICA512–GFP, were expressed in resting (*R*) and glucose-stimulated (*S*) INS-1 cells, which were lysed for analysis of the fusion proteins by immunoblotting. Upon glucose stimulation, synthesis of both ICA512–GFP and ΔRESP18HD ICA512–GFP proforms was upregulated (Fig. 9, lanes 2 and 6). As shown by our previous work [5,24], the proprotein-convertase-cleaved ICA512–TMF–GFP, generated upon SG maturation, was readily detectable in resting cells (Fig. 9, lane 1), but not in the stimulated cells, due to its depletion upon the cytoplasmic domain calpain-dependent cleavage upon granule exocytosis at the cell surface (Fig. 9, lane 2).

The expression pattern of ΔRESP18HD ICA512–GFP was radically different. ΔRESP18HD proICA512–GFP accumulated comparably in much large amounts than proICA512–GFP in both resting and stimulated cells (Fig. 9, lanes 5 and 6). Nonetheless, a minor fraction of ΔRESP18HD proICA512–GFP was also undergoing conversion to a fragment of similar size to that generated by proICA512–GFP to ICA512–TMF–GFP conversion (Fig. 9, lanes 1 and 5). Furthermore, ICA512–TMF–GFP originating from ΔRESP18HD proICA512–GFP, like ICA512–TMF–GFP generated from proICA512–GFP, was also depleted upon stimulation. Site-directed mutagenesis of the proprotein convertase cleavage site sequence of ICA512–GFP and ΔRESP18HD ICA512–GFP, introducing a S449V replacement at the position +1 following the sequence of the dibasic lysine motif, impaired the generation of ICA512–TMF–GFP (Fig. 9, lanes 1/3 and 5/7) from both ΔRESP18HD and wild type ICA512–GFP, again indicating that in INS-1 cells ΔRESP18HD proICA512–GFP is, at least to some extent, converted in a similar manner as proICA512–GFP in INS-1 cells.

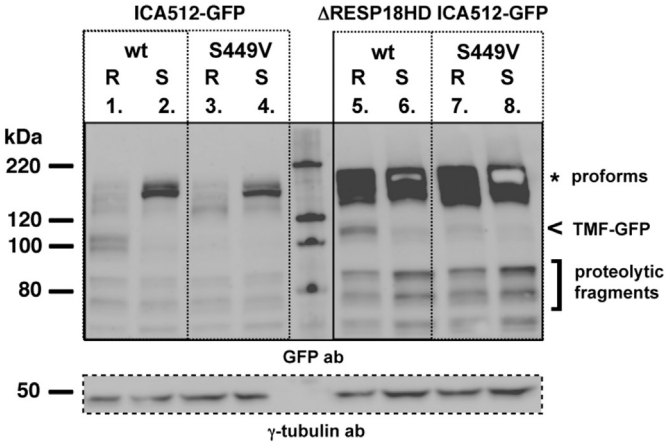

Fig. 9. ICA512–GFP and ΔRESP18HD ICA512–GFP expression and conversion. Immunoblotting for GFP in lysates of resting (*R*) or stimulated (*S*) INS-1 cells expressing ICA512–GFP or ΔRESP18HD ICA512–GFP wild type (*wt*) forms or their proprotein convertase site, (*S449V*), mutants. The corresponding proforms are indicated with an asterisk and the proprotein convertase generated ICA512–TMF–GFP forms with an arrowhead. For normalization, the lysates were also immunoblotted for γ-tubulin.

The above results imply that a small fraction of ΔRESP18HD proICA512–GFP might be sorted to premature SGs. Therefore, we investigated its localization in comparison with ICA512-GFP by immunostaining of the cells for insulin. Unlike ICA512–GFP, which co-localized with the punctuated staining of insulin SGs in both resting and stimulated cells (Fig. 10, Panel A, lower images), only a minor fraction of ΔRESP18HD ICA512–GFP signal was found overlapping with punctuated SGs like signal (Fig. 10, Panel A, upper images). ΔRESP18HD ICA512–GFP or ICA512–GFP expressing cells in resting or glucose-stimulation media were also incubated with antibodies directed to the ICA512 mature ectodomain (*ME ICA512*). The cells were fixed and stained without permeabilization with the secondary antibodies to examine exposure of ΔRESP18HD ICA512–GFP and ICA512–GFP. Consistently with previous findings [5,24], ICA512-GFP was detectable at the cell surface only in the glucose-stimulated cells (Fig. 10, Panel B, lower right images). In contrast, ΔRESP18HD ICA512–GFP was exposed extracellularly in both resting and glucose stimulated cells (Fig. 10 Panel B, upper left and right images). Since the behavior of ICA512–GFP results from its sorting into insulin SGs and regulated exocytosis, the contrasting behavior of ΔRESP18HD ICA512–GFP indicates that lack of RESP18HD impairs most of the protein from being sorted to insulin SGs and inserted to the plasma membrane in a regulated fashion.

4. Discussion

Although ICA512–RESP18HD can be considered a structural unit due to its conservation in distinct protein families, direct evidence for its functioning and properties has been lacking. By preparing pure ICA512–RESP18HD and characterizing its biophysical and biochemical properties in vitro we are now in better position to undertake the study of its biological function on a structural basis.

A prominent feature of isolated ICA512–RESP18HD is its conformational plasticity. Whereas CD and intrinsic fluorescence showed that ICA512–RESP18HD displays distinct secondary and tertiary structures, its solubility is limited and restricted to acidic conditions, compatible with the lumenal pH of the mature SG. Thus, at neutral pH, pure ICA512–RESP18HD readily forms insoluble oligomers. The ionization profile, with charge close to zero at neutral pH, is certainly an important factor explaining the low solubility of ICA512–RESP18HD. However, the presence of a short intrinsically disordered sequence at its C-terminus – which is also conserved in RESP18 and in the corresponding region of phogrin – must also contribute to its tendency to aggregate. The ANS binding results confirm that the isolated protein exposes hydrophobic patches that may enhance intermolecular interactions and hence aggregation. Thus, the conformational state of isolated ICA512–RESP18HD can be considered a dynamic combination of folded and partially folded structures with the potential to adjust to changes in the medium or in the presence of interacting molecules.

Further evidence for the propensity to association is the easiness of intermolecular disulfide formation exhibited by ICA512–RESP18HD. Although the results show that oxidation is not a requirement for ICA512–RESP18HD incipient oligomerization, the formation of disulfide bridges can consolidate the aggregates making the process irreversible. We show that the cysteine residues of ICA512–RESP18HD are highly conserved among the R8 subtype of RPTPs (Fig. 1, Panel D), which points to their functional and structural importance. In addition, we provide here evidence that the tendency to form disulfide-linked high-order aggregates is due to an unusually high reactivity in thiol–disulfide exchange reactions. All together, the conformational plasticity, the tendency to form disulfide bridges, the tendency for association, and the pH-dependent aggregation hint to the participation of ICA512–RESP18HD in the dynamic network of interactions deemed fundamental for sorting to the SG and regulated secretion, particularly in concert with other proteins prone to form high order aggregates [12].

The biophysical properties of ICA512–RESP18HD prompted the question as if this domain can act as a recognition module. We started

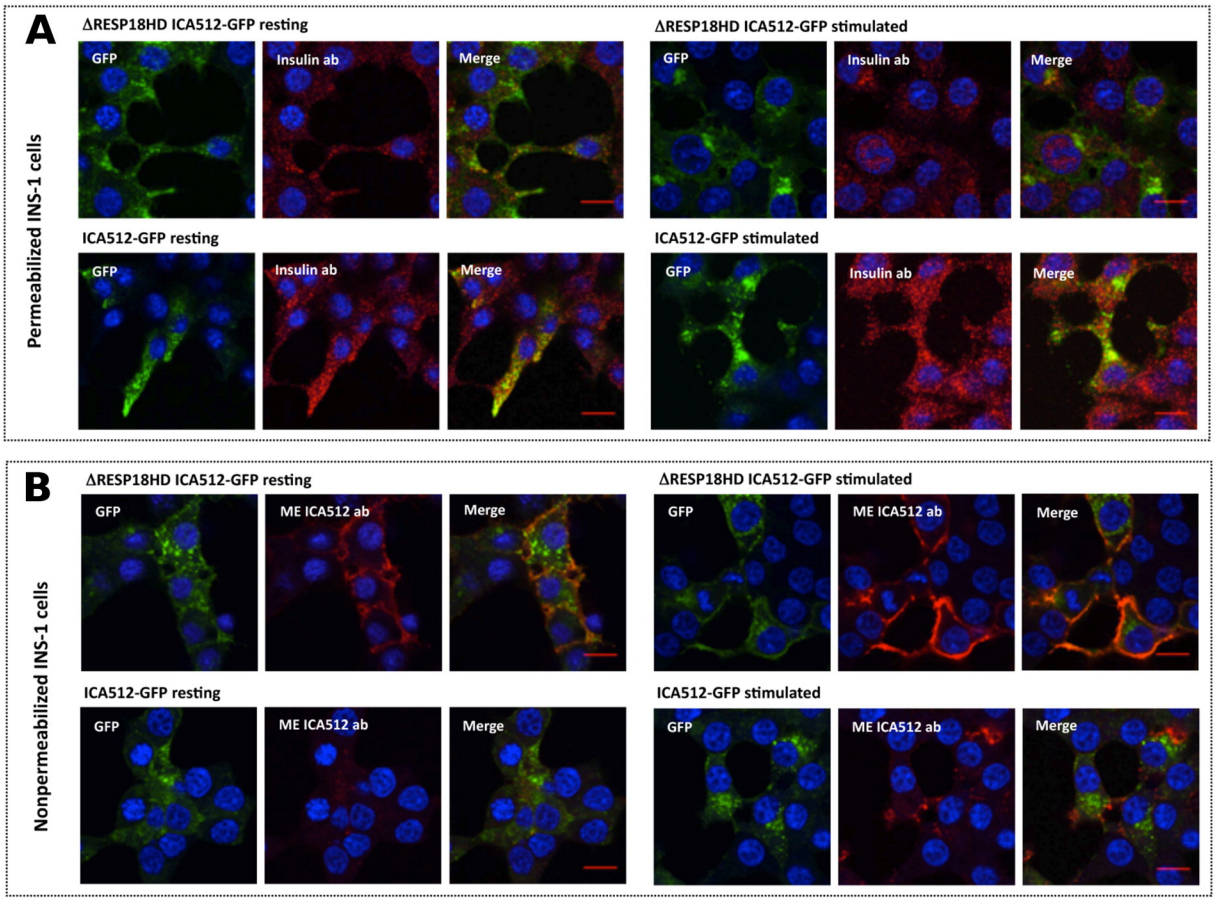

Fig. 10. ICA512–GFP and ΔRESP18HD ICA512–GFP targeting. Confocal microscopy images of (A) permeabilized and (B) nonpermeabilized INS-1 cells expressing ΔRESP18HD ICA512–GFP or ICA512–GFP (within each panel, upper and lower rows, respectively). Green fluorescence corresponds to GFP. Red fluorescence corresponds to (A) insulin SGs immunostaining or (B) surface exposed ICA512 immunostained with ME ICA512 antibody directed against the ICA512 mature proximal ectodomain. Merge color images, with the scale bars = 10 μm, are shown on the right. Cell nuclei are shown by DAPI staining, in blue. $n = 3$. (A) ICA512–GFP co-localized with the punctuated staining of insulin SGs in both resting and stimulated cells. (B, lower right) ICA512-GFP was detectable at the cell surface only in glucose-stimulated cells (B, upper left and right). Contrastingly, ΔRESP18HD ICA512–GFP was exposed extracellularly in both resting and glucose-stimulated cells.

to test this hypothesis and found evidence of binding to proinsulin and insulin. The affinity of the interaction was in the low micromolar range, similar to that of insulin interacting with insulin antibodies elicited during replacement therapy in diabetic patients [37]. It is widely accepted that such affinity exhibited by specific antibodies is compatible with the efficient binding and opsonization of the antigen. Thus, it is reasonable to infer that ICA512–RESP18HD may actually be complexed to a similar extent by insulin in vivo.

The significance of the interaction between ICA512–RESP18HD and insulin/proinsulin must be considered in the context of other known protein interactions suggested for ICA512. The cytoplasmic domain of ICA512 interacts with over a dozen of cytosolic proteins [38–42]. For many of these interactions, a connection with cellular mechanisms was inferred and for some of them, direct experimental evidence of their significance is available [12]. On the other hand, reports of interactions of the lumenal domains of ICA512 are lacking. Conceivably, the reported binding of carboxypeptidase E to a lumenal region of phogrin [43] also takes place for ICA512, as also suggested by preliminary evidence (our unpublished observations). It was proposed that the lumenal interaction between phogrin and carboxypeptidase E is involved in their mutual sorting from the TGN to the SG [43]. The interaction between ICA512–RESP18HD and proinsulin/insulin unveiled in this work might contribute to phase separation (demixing) of micro-domains or high-order multiprotein assemblies for sorting and trafficking through the regulated pathway [44–48]. In this capacity, the flexible nature of regions lacking well-defined structures could allow ICA512–RESP18HD binding to multiple targets. In this respect it should be considered that the proteins including a RESP18 domain are widely expressed in neuroendocrine cells, and thus presumably interacting with various cargo proteins.

In a previous study we demonstrated that the removal of the NTF domain (Fig. 1; residues 34 to 449) aborts targeting of proICA512 to SGs [24]. There, we also demonstrated that ICA512–RESP18HD tagged with GFP (i.e. residues 34 to 131 of NTF followed by GFP) is directed to the SG, whereas ICA512–NTF tagged with GFP is rather retained in the ER. We now strengthen those findings by showing that the removal of RESP18HD suffices to preclude most of ΔRESP18HD ICA512–GFP from being sorted to the SG, thereby diverting it instead to the constitutive pathway and thus resulting in its accumulation at the cell surface. All these findings, along with the biophysical and biochemical evidence discussed above, start to delineate a prominent role of ICA512–RESP18HD for driving the parent protein and granule cargoes, from the ER and Golgi membrane compartments to the mature SGs.

Additional research will be necessary to establish the mechanisms by which ICA512–RESP18HD participates in the targeting of the receptor to secretory granules. However, and as a working hypothesis, the process may be envisaged as follows. ICA512–RESP18HD would contain a granule-directing determinant, which is only effective when a second determinant for ER retention is overcome. Such ER retention signal would be located within a contiguous region of the receptor with high potential for structural disorder (within residues 132 to 449 of the NTF). ICA512 retention in the ER can be overcome experimentally by deletion, as in the case of ΔNTF ICA512–GFP and ΔRESP18HD ICA512–GFP or in vivo by a more sophisticated interplay of the extracellular/

luminal domain and other SG protein interactions. Conceivably, the silencing of the ER retention signal might involve its folding in concert with the other parts of the receptor.

Transparency document

The Transparency document associated with this article can be found, in online version.

Acknowledgments

This work was supported by the Consejo Nacional de Investigaciones Científicas y Técnicas, the Agencia Nacional de Promoción Científica y Tecnológica, and the Universidad Nacional de Quilmes to ME, and by the Network of Competence for Diabetes Mellitus (grant FKZ:01GI1102) and the German Center for Diabetes Research (DZD e.V.) supported by the German Ministry for Education and Research to MS. The collaboration between the Ermácora and the Solimena teams was supported by the German–Argentina DFG Exchange program (grant 444 ARG113/9/10).

References

[1] J.N. Andersen, O.H. Mortensen, G.H. Peters, P.G. Drake, L.F. Iversen, O.H. Olsen, P.G. Jansen, H.S. Andersen, N.K. Tonks, N.P. Moller, Structural and evolutionary relationships among protein tyrosine phosphatase domains, Mol. Cell. Biol. 21 (2001) 7117–7136.
[2] J.N. Andersen, P.G. Jansen, S.M. Echwald, O.H. Mortensen, T. Fukada, R. Del Vecchio, N.K. Tonks, N.P. Moller, A genomic perspective on protein tyrosine phosphatases: gene structure, pseudogenes, and genetic disease linkage, FASEB J. 18 (2004) 8–30.
[3] G. Magistrelli, S. Toma, A. Isacchi, Substitution of two variant residues in the protein tyrosine phosphatase-like PTP35/IA-2 sequence reconstitutes catalytic activity, Biochem. Biophys. Res. Commun. 227 (1996) 581–588.
[4] S. Torii, Expression and function of IA-2 family proteins, unique neuroendocrine-specific protein-tyrosine phosphatases, Endocr. J. 56 (2009) 639–648.
[5] M. Solimena, R.J. Dirkx, J.M. Hermel, S. Pleasic-Williams, J.A. Shapiro, L. Caron, D.U. Rabin, ICA 512, an autoantigen of type I diabetes, is an intrinsic membrane protein of neurosecretory granules, EMBO J. 15 (1996) 2102–2114.
[6] C. Wasmeier, J.C. Hutton, Molecular cloning of phogrin, a protein-tyrosine phosphatase homologue localized to insulin secretory granule membranes, J. Biol. Chem. 271 (1996) 18161–18170.
[7] M. Trajkovski, H. Mziaut, A. Altkrüger, J. Ouwendijk, K. Knoch, S. Müller, M. Solimena, Nuclear translocation of an ICA512 cytosolic fragment couples granule exocytosis and insulin expression in beta-cells, J. Cell Biol. 167 (2004) 1063–1074.
[8] M. Trajkovski, H. Mziaut, S. Schubert, Y. Kalaidzidis, A. Altkrüger, M. Solimena, Regulation of insulin granule turnover in pancreatic beta-cells by cleaved ICA512, J. Biol. Chem. 283 (2008) 33719–33729.
[9] H. Mziaut, S. Kersting, K. Knoch, W. Fan, M. Trajkovski, K. Erdmann, H. Bergert, F. Ehehalt, H. Saeger, M. Solimena, ICA512 signaling enhances pancreatic beta-cell proliferation by regulating cyclins D through STATs, Proc. Natl. Acad. Sci. U. S. A. 105 (2008) 674–679.
[10] S. Torii, N. Saito, A. Kawano, N. Hou, K. Ueki, R.N. Kulkarni, T. Takeuchi, Gene silencing of phogrin unveils its essential role in glucose-responsive pancreatic beta-cell growth, Diabetes 58 (2009) 682–692.
[11] S. Schubert, K. Knoch, J. Ouwendijk, S. Mohammed, Y. Bodrov, M. Jäger, A. Altkrüger, C. Wegbrod, M.E. Adams, Y. Kim, S.C. Froehner, O.N. Jensen, Y. Kalaidzidis, M. Solimena, β2-Syntrophin is a Cdk5 substrate that restrains the motility of insulin secretory granules, PLoS One 5 (2010), e12929.
[12] J. Suckale, M. Solimena, The insulin secretory granule as a signaling hub, Trends Endocrinol. Metab. 21 (2010) 599–609.
[13] J. Lu, Q. Li, H. Xie, Z.J. Chen, A.E. Borovitskaya, N.K. Maclaren, A.L. Notkins, M.S. Lan, Identification of a second transmembrane protein tyrosine phosphatase, IA-2beta, as an autoantigen in insulin-dependent diabetes mellitus: precursor of the 37-kDa tryptic fragment, Proc. Natl. Acad. Sci. U. S. A. 93 (1996) 2307–2311.
[14] G.F. Bottazzo, E. Bosi, C.A. Cull, E. Bonifacio, M. Locatelli, P. Zimmet, I.R. Mackay, R.R. Holman, IA-2 antibody prevalence and risk assessment of early insulin requirement in subjects presenting with type 2 diabetes, Diabetologia 48 (2005) 703–708.
[15] K. Saeki, M. Zhu, A. Kubosaki, J. Xie, M.S. Lan, A.L. Notkins, Targeted disruption of the protein tyrosine phosphatase-like molecule IA-2 results in alterations in glucose tolerance tests and insulin secretion, Diabetes 51 (2002) 1842–1850.
[16] A. Kubosaki, S. Gross, J. Miura, K. Saeki, M. Zhu, S. Nakamura, W. Hendriks, A.L. Notkins, Targeted disruption of the IA-2beta gene causes glucose intolerance and impairs insulin secretion but does not prevent the development of diabetes in NOD mice, Diabetes 53 (2004) 1684–1691.
[17] J. Henquin, M. Nenquin, A. Szollosi, A. Kubosaki, A.L. Notkins, Insulin secretion in islets from mice with a double knockout for the dense core vesicle proteins islet antigen-2 (IA-2) and IA-2beta, J. Endocrinol. 196 (2008) 573–581.
[18] A. Kubosaki, S. Nakamura, A.L. Notkins, Dense core vesicle proteins IA-2 and IA-2beta: metabolic alterations in double knockout mice, Diabetes 54 (Suppl. 2) (2005) S46–S51.
[19] J. Seissler, T.B. Nguyen, G. Aust, H. Steinbrenner, W.A. Scherbaum, Regulation of the diabetes-associated autoantigen IA-2 in INS-1 pancreatic beta-cells, Diabetes 49 (2000) 1137–1141.
[20] C. Roberts, G.A. Roberts, K. Löbner, M. Bearzatto, A. Clark, E. Bonifacio, M.R. Christie, Expression of the protein tyrosine phosphatase-like protein IA-2 during pancreatic islet development, J. Histochem. Cytochem. 49 (2001) 767–776.
[21] S. Shimizu, N. Saito, A. Kubosaki, S. SungWook, N. Takeyama, T. Sakamoto, Y. Matsumoto, K. Saeki, Y. Matsumoto, T. Onodera, Developmental expression and localization of IA-2 mRNA in mouse neuroendocrine tissues, Biochem. Biophys. Res. Commun. 288 (2001) 165–171.
[22] H. Steinbrenner, T. Nguyen, U. Wohlrab, W.A. Scherbaum, J. Seissler, Effect of proinflammatory cytokines on gene expression of the diabetes-associated autoantigen IA-2 in INS-1 cells, Endocrinology 143 (2002) 3839–3845.
[23] K. Löbner, H. Steinbrenner, G.A. Roberts, Z. Ling, G. Huang, S. Piquer, D.G. Pipeleers, J. Seissler, M.R. Christie, Different regulated expression of the tyrosine phosphatase-like proteins IA-2 and phogrin by glucose and insulin in pancreatic islets: relationship to development of insulin secretory responses in early life, Diabetes 51 (2002) 2982–2988.
[24] J.M. Torkko, M.E. Primo, R. Dirkx, A. Friedrich, A. Viehrig, E. Vergari, B. Borgonovo, A. Sonmez, C. Wegbrod, M. Lachnit, C. Munster, M.P. Sica, M.R. Ermacora, M. Solimena, Stability of proICA512/IA-2 and its targeting to insulin secretory granules require beta4-sheet-mediated dimerization of its ectodomain in the endoplasmic reticulum, Mol. Cell. Biol. 35 (2015) 914–927.
[25] H. Mziaut, M. Trajkovski, S. Kersting, A. Ehninger, A. Altkrüger, R.P. Lemaitre, D. Schmidt, H. Saeger, M. Lee, D.N. Drechsel, S. Müller, M. Solimena, Synergy of glucose and growth hormone signalling in islet cells through ICA512 and STAT5, Nat. Cell Biol. 8 (2006) 435–445.
[26] M.R. Schiller, R.E. Mains, B.A. Eipper, A novel neuroendocrine intracellular signaling pathway, Mol. Endocrinol. 11 (1997) 1846–1857.
[27] M. Liang, J.L. Yang, M.J. Bian, J. Liu, X.Q. Hong, Y.C. Wang, Y.F. Huang, S.P. Gu, M. Yu, F. Huang, J. Fei, Requirement of regulated endocrine-specific protein-18 for development and expression of regulated endocrine-specific protein-18 isoform c in mice, Mol. Biol. Rep. 38 (2011) 2557–2562.
[28] G. Zhang, H. Hirai, T. Cai, J. Miura, P. Yu, H. Huang, M.R. Schiller, W.D. Swaim, R.D. Leapman, A.L. Notkins, RESP18, a homolog of the luminal domain IA-2, is found in dense core vesicles in pancreatic islet cells and is induced by high glucose, J. Endocrinol. 195 (2007) 313–321.
[29] H. Schägger, G. von Jagow, Tricine-sodium dodecyl sulfate-polyacrylamide gel electrophoresis for the separation of proteins in the range from 1 to 100 kDa, Anal. Biochem. 166 (1987) 368–379.
[30] Y. Nozaki, Determination of tryptophan, tyrosine, and phenylalanine by second derivative spectrophotometry, Arch. Biochem. Biophys. 277 (1990) 324–333.
[31] R. Development Core Team, R: a Language and Environment for Statistical Computing, R Foundation for Statistical Computing, Vienna, Austria, 2012 (ISBN 3-900051-07-0. http://www.R-project.org/).
[32] C.K. Riener, G. Kada, H.J. Gruber, Quick measurement of protein sulfhydryls with Ellman's reagent and with 4,4′-dithiodipyridine, Anal. Bioanal. Chem. 373 (2002) 266–276.
[33] G.V. Semisotnov, N.A. Rodionova, O.I. Razgulyaev, V.N. Uversky, A.F. Gripas, R.I. Gilmanshin, Study of the "molten globule" intermediate state in protein folding by a hydrophobic fluorescent probe, Biopolymers 31 (1991) 119–128.
[34] M. Sickmeier, J.A. Hamilton, T. LeGall, V. Vacic, M.S. Cortese, A. Tantos, B. Szabo, P. Tompa, J. Chen, V.N. Uversky, Z. Obradovic, A.K. Dunker, DisProt: the database of disordered proteins, Nucleic Acids Res. 35 (2007) D786–D793.
[35] G.B. Kallis, A. Holmgren, Differential reactivity of the functional sulfhydryl groups of cysteine-32 and cysteine-35 present in the reduced form of thioredoxin from *Escherichia coli*, J. Biol. Chem. 255 (1980) 10261–10265.
[36] Z. Shaked, R.P. Szajewski, G.M. Whitesides, Rates of thiol-disulfide interchange reactions involving proteins and kinetic measurements of thiol pKa values, Biochemistry 19 (1980) 4156–4166.
[37] A. Trabucchi, R.F. Iacono, L.L. Guerra, N.I. Faccinetti, A.G. Krochik, M.C. Arriazu, E. Poskus, S.N. Valdez, Characterization of insulin antibodies by Surface Plasmon Resonance in two clinical cases: brittle diabetes and insulin autoimmune syndrome, PLoS One 8 (2013), e84099.
[38] Y.F. Hu, H.L. Zhang, T. Cai, S. Harashima, A.L. Notkins, The IA-2 interactome, Diabetologia 48 (2005) 2576–2581.
[39] S. Gross, C. Blanchetot, J. Schepens, S. Albet, R. Lammers, J. den Hertog, W. Hendriks, Multimerization of the protein-tyrosine phosphatase (PTP)-like insulin-dependent diabetes mellitus autoantigens IA-2 and IA-2beta with receptor PTPs (RPTPs). Inhibition of RPTPalpha enzymatic activity, J. Biol. Chem. 277 (2002) 48139–48145.
[40] S. Berghs, D. Aggujaro, R.J. Dirkx, E. Maksimova, P. Stabach, J.M. Hermel, J.P. Zhang, W. Philbrick, V. Slepnev, T. Ort, M. Solimena, Beta IV spectrin, a new spectrin localized at axon initial segments and nodes of ranvier in the central and peripheral nervous system, J. Cell Biol. 151 (2000) 985–1002.
[41] T. Ort, S. Voronov, J. Guo, K. Zawalich, S.C. Froehner, W. Zawalich, M. Solimena, Dephosphorylation of beta-2-syntrophin and Ca^{2+}/mu-calpain-mediated cleavage of ICA512 upon stimulation of insulin secretion, EMBO J. 20 (2001) 4013–4023.
[42] T. Rolland, M. Tasan, B. Charloteaux, S.J. Pevzner, Q. Zhong, N. Sahni, S. Yi, I. Lemmens, C. Fontanillo, R. Mosca, A. Kamburov, S.D. Ghiassian, X. Yang, L. Ghamsari, D. Balcha, B.E. Begg, P. Braun, M. Brehme, M.P. Broly, A. Carvunis, D. Convery-Zupan, R. Corominas, J. Coulombe-Huntington, E. Dann, M. Dreze, A. Dricot, C. Fan, E. Franzosa, F. Gebreab, B.J. Gutierrez, M.F. Hardy, M. Jin, S. Kang, R. Kiros, G.N. Lin, K. Luck, A. MacWilliams, J. Menche, R.R. Murray, A. Palagi, M.M.

Poulin, X. Rambout, J. Rasla, P. Reichert, V. Romero, E. Ruyssinck, J.M. Sahalie, A. Scholz, A.A. Shah, A. Sharma, Y. Shen, K. Spirohn, S. Tam, A.O. Tejeda, S.A. Trigg, J. Twizere, K. Vega, J. Walsh, M.E. Cusick, Y. Xia, A. Barabási, L.M. Iakoucheva, P. Aloy, J. De Las Rivas, J. Tavernier, M.A. Calderwood, D.E. Hill, T. Hao, F.P. Roth, M. Vidal, A proteome-scale map of the human interactome network, Cell 159 (2014) 1212–1226.

[43] N. Saito, T. Takeuchi, A. Kawano, M. Hosaka, N. Hou, S. Torii, Luminal interaction of phogrin with carboxypeptidase E for effective targeting to secretory granules, Traffic 12 (2011) 499–506.

[44] A.A. Hyman, K. Simons, Cell biology. Beyond oil and water-phase transitions in cells, Science 337 (2012) 1047–1049.

[45] J. Li, T. McQuade, A.B. Siemer, J. Napetschnig, K. Moriwaki, Y. Hsiao, E. Damko, D. Moquin, T. Walz, A. McDermott, F.K. Chan, H. Wu, The RIP1/RIP3 necrosome forms a functional amyloid signaling complex required for programmed necrosis, Cell 150 (2012) 339–350.

[46] H. Wu, Higher-order assemblies in a new paradigm of signal transduction, Cell 153 (2013) 287–292.

[47] N. Kedersha, P. Ivanov, P. Anderson, Stress granules and cell signaling: more than just a passing phase? Trends Biochem. Sci. 38 (2013) 494–506.

[48] P.E. Wright, H.J. Dyson, Intrinsically disordered proteins in cellular signalling and regulation, Nat. Rev. Mol. Cell Biol. 16 (2015) 18–29.

[49] V.N. Uversky, Use of fast protein size-exclusion liquid chromatography to study the unfolding of proteins which denature through the molten globule, Biochemistry 32 (1993) 13288–13298.